Published in final edited form as:

Dev Neurobiol. 2016 February ; 76(2): 137–149. doi:10.1002/dneu.22304.

Differences in CART expression and cell cycle behaviour discriminate sympathetic neuroblast from chromaffin cell lineages in mouse sympathoadrenal cells

Wing Hei Chan[1], **David G Gonsalvez**[1], **Heather M Young**[1], **E. Michelle Southard-Smith**[2], **Kylie N Cane**[1], **Colin R Anderson**[1]

[1]Department of Anatomy and Neuroscience, University of Melbourne, Victoria 3010, Australia

[2]Division of Genetic Medicine, Department of Medicine, Vanderbilt University School of Medicine, 529 Light Hall, 2215 Garland Avenue, Nashville, Tennessee

Abstract

Adrenal medullary chromaffin cells and peripheral sympathetic neurons originate from a common sympathoadrenal (SA) progenitor cell. The timing and phenotypic changes that mark this lineage diversification are not fully understood. The present study investigated the expression patterns of phenotypic markers, and cell cycle dynamics, in the adrenal medulla and the neighbouring suprarenal ganglion of embryonic mice. The noradrenergic marker, tyrosine hydroxylase (TH), was detected in both presumptive adrenal medulla and sympathetic ganglion cells, but with significantly stronger immunostaining in the former. There was intense cocaine and amphetamine-regulated transcript (CART) peptide immunostaining in most neuroblasts, whereas very few adrenal chromaffin cells showed detectable CART immunostaining. This phenotypic segregation appeared as early as E12.5, before anatomical segregation of the two cell types. Cell cycle dynamics were also examined. Initially, 88% of Sox10 positive (+) neural crest progenitors were proliferating at E10.5. Many SA progenitor cells withdrew from the cell cycle at E11.5 as they started to express TH. Whereas 70% of neuroblasts (TH+/CART+ cells) were back in the cell cycle at E12.5, only around 20% of chromaffin (CART negative) cells were in the cell cycle at E12.5 and subsequent days. Thus, chromaffin cell and neuroblast lineages showed differences in proliferative behaviour from their earliest appearance. We conclude that the intensity of TH immunostaining and the expression of CART permit early discrimination of chromaffin cells and sympathetic neuroblasts, and that developing chromaffin cells exhibit significantly lower proliferative activity relative to sympathetic neuroblasts.

Keywords

Phenotypic lineage marker; Sympathoadrenal cells; Cell cycle dynamic; Cocaine and amphetamine-regulated transcript (CART) peptide; Adrenal chromaffin cells

Corresponding Author: Wing Hei Chan, Department of Anatomy and Neuroscience, The University of Melbourne, VIC 3010, Australia. chanwh@student.unimelb.edu.au.

Introduction

The neural crest (NC) gives rise to a range of cell types including, sympathetic neurons and both intra- and extra-adrenal chromaffin cells (Landis and Patterson, 1981; Anderson, 1993; Schober et al., 2000). Sympathetic neurons and adrenal chromaffin cells appear to originate from a common precursor, the sympathoadrenal (SA) progenitor cell (Anderson and Axel, 1986; Anderson, 1993; Francis and Landis, 1999; Langley and Grant, 1999; Huber et al., 2002; Ernsberger et al., 2005; Unsicker et al., 2005; Shtukmaster et al., 2013; Lumb and Schwarz, 2015). Multipotent NC cells delaminate from the trunk neural tube and migrate ventrolaterally through the anterior parts of somites to the vicinity of the dorsal aorta (Landis and Patterson, 1981; Bronner-Fraser, 1994; Anderson, 1997; Shtukmaster et al., 2013). Bone morphogenetic proteins (BMPs) produced from the dorsal aorta induce the expression of neuregulin 1 and CXCL12 in local mesenchyme to regulate cell migration and lineage separation in SA cells (Saito et al., 2012). SA cells express catecholaminergic synthetic enzymes, including tyrosine hydroxylase (TH) and dopamine β hydroxylase (DβH) and, initially, the neuronal markers Tuj1, PGP9.5 and Hu (Huber, 2006; Shtukmaster et al., 2013). Subsets of SA cells located ventrolateral to the dorsal aorta at abdominal levels then differentiate into either sympathetic neurons or chromaffin cells and coalesce into sympathetic ganglia and the adrenal medulla respectively (Landis and Patterson, 1981; Huber, 2006; Saito et al., 2012; Lumb and Schwarz, 2015).

Many components of the transcriptional network underlying the development of the SA cell lineage have been identified. In migrating NC cells in mouse, SoxE transcription factors (Sox8, Sox9 and Sox10) are expressed after delamination from the neural tube (Cheung et al., 2005; Morikawa et al., 2007; Reiprich et al., 2008; Huber et al., 2009). Around the aorta, BMPs trigger the expression of a network of transcription factors in NC-derived cells including Ascl1, Phox2b, Phox2a, Insm1, Hand2 and Gata2/3 (Tsarovina et al., 2004; Callahan et al., 2008; Wildner et al., 2008; Rohrer, 2011). These transcription factors generate and maintain the catecholaminergic phenotype and neuronal properties during differentiation of SA cells (Pattyn et al., 1999; Stanke et al., 2004; Tsarovina et al., 2004; Huber et al., 2005). However, none of these factors seem to explain the generation of separate chromaffin and neuronal cells as both cell types express the same transcription factors during their early development. MicroRNAs may be important in defining the two SA lineages as judged from the effect of deletion of Dicer 1, a microRNA processing ribonuclease (Stubbusch et al., 2013).

Mature sympathetic neurons and adrenal chromaffin cells exhibit distinct morphological and functional traits. Sympathetic ganglionic neurons are multipolar cells with several branching dendrites and an axon projecting over long distances for signal transmission (Gabella, 2001). Mature adrenal chromaffin cells are columnar or polygonal endocrine cells with large secretory vesicles storing catecholamines (Waring, 1936; Cuchillo-Ibanez et al., 1999). Mammalian sympathetic neurons synthesise and release noradrenaline as a neurotransmitter, but a sub-population of adrenal chromaffin cells also synthesises adrenaline using phenylethanolamine N-methyltransferase (PNMT) to methylate noradrenaline to adrenaline. The rate of overall catecholamine production is much higher in chromaffin tissue than in

sympathetic neurons (Wurtman and Axelrod, 1966; Kannan, 1986) and the relative levels of TH immunoreactivity seem to reflect this (Schober et al., 2013).

The aim of the current study was to identify helpful marker(s) for the discrimination of neuroblasts and chromaffin cells as they differentiate, which would facilitate future investigation of the mechanisms underlying the differentiation and proliferation of the two main cells types in the SA lineage. In the mouse, adrenal chromaffin cells can be readily distinguished from sympathetic neuroblasts from E13.5 based on their anatomical arrangement (Stubbusch et al., 2013). However, at younger ages it is difficult to distinguish the two lineages. A range of neuronal markers which, later in development, are restricted to neurons, are expressed transiently in E12.5 SA cells (Stubbusch et al., 2013; Unsicker et al., 2013). SCG10 expression allows separation of the two lineages at E12.5 (Stubbusch et al., 2013), but other means to distinguish the cell types prior to their anatomical separation would be valuable. In this study, we analysed the temporal and spatial expression patterns of TH and PNMT, along with the neuropeptide, cocaine and amphetamine regulated transcript (CART), to determine if SA cells can be separated into two lineages. CART is expressed by subpopulations of neurons in the CNS, the peripheral nervous system and by some chromaffin cells (Dun et al., 2000; Gonsalvez et al., 2010), and is expressed early in the developing enteric nervous system (Heanue and Pachnis, 2006, M.S.-S. unpublished observation). As cell cycle changes often accompany differentiation of more mature cell types from progenitor cells in the nervous system (Caviness et al., 2003; Cheffer et al., 2013), including the paravertebral sympathetic ganglia (Gonsalvez et al., 2013), we also analysed the proliferative behaviour of SA cells and their derivatives. Our data show that chromaffin cells and sympathetic neuroblasts can be discriminated by differences in the intensity of TH immunostaining, expression of CART and proliferative activity.

Materials and Methods

Animals

All animal experiments were approved by the University of Melbourne Animal Experimentation Ethics committee and complied with National Health & Medical Research Council of Australia (NHMRC) guidelines. Wild-type C57BL/6 mice were time plug-mated and the morning of detection of the plug was counted as embryonic day (E) 0.5.

Dual S-phase Labelling

The S-phase labelling index and S-phase length were obtained by a dual S-phase marker labelling technique as described by Gonsalvez et al. (2013; 2014). Briefly, pregnant dams between 10.5–16.5 days post-fertilization were injected intraperitoneally with the first S-phase marker, bromodeoxyuridine (BrdU; Roche Diagnostics), at 100 μg/g body weight followed, 2 hours later, by the second S-phase marker, ethyldeoxyuridine (EdU; Invitrogen) at 50 μg/g body weight. After a further 30 minutes, the dams were killed and embryos were collected for immunohistochemistry analysis.

Immunohistochemistry and Imaging

Pregnant dams were killed by cervical dislocation and the embryos were collected and decapitated. The body was divided between the thorax and abdomen and the abdomen fixed overnight in Zamboni's fixative (2% formaldehyde and 15% saturated picric acid in 0.1M phosphate buffer, pH 7.4, composition in mM; Na_2PO_4, 75; $NaH_2PO_4{\cdot}2H_2O$, 25). Fixed embryos were then washed, and stored in 20% sucrose solution at 4°C. Embryos were then embedded in OCT (TissueTek) and snap frozen in liquid nitrogen-cooled isopentane. Transverse sections of the abdominal region containing the adrenal were cut on a cryostat at 10 μm thickness.

Sections were collected as separate, one in four series. One series of sections was processed overnight with primary antisera. Initially, a combination of chicken anti-TH (1:100, Millipore), rabbit anti-CART (1:200, Phoenix Pharmaceuticals), and sheep anti-PNMT (1:500, Howe) was used. After washing in phosphate buffered saline (PBS, composition in mM; NaCl, 145; Na_2PO_4, 7.5; $NaH_2PO_4{\cdot}2H_2O$, 2.5) the bound primary antisera were visualized after two hours incubation with secondary antisera: donkey anti-chicken FITC (1:100, Jackson ImmunoResearch), donkey anti-rabbit Dylight594 (1:500, Jackson ImmunoResearch), and donkey anti-sheep Alexa Fluor647 (1:200, Invitrogen) and the nuclei were stained with bisbenzimide (I μg/ml, Hoechst 33446).

The second and third series of sections from each embryo were processed for S-phase labelling. Sections from E10.5–12.5 embryos were processed for TH and either CART or Sox10 (goat anti-Sox10; 1:100, R&D Systems) immunostaining respectively. The bound primary antisera were visualized by two hours incubation with secondary antisera: donkey anti-chicken Alexa Fluor647 (1:200, Invitrogen) and either donkey anti-rabbit biotin (1:400, Jackson) or donkey anti-sheep biotin (1:200, Jackson ImmunoResearch) respectively and 1 hour tertiary step with streptavidin conjugated to Dylight405 (1:100, Jackson ImmunoResearch). Sections from E13.5-E16.5 embryos were processed for CART and PNMT with or without TH respectively. For series with TH, the bound primary antisera were visualized by secondary antisera: donkey anti-chicken Alexa Fluor647, donkey anti-rabbit biotin, donkey anti-sheep biotin and a tertiary step with streptavidin conjugated to Dylight405 for CART and PNMT. For sections without TH, the bound primary antisera were visualized by secondary antisera: donkey anti-rabbit biotin, donkey anti-sheep Alexa Fluor647 and tertiary step with streptavidin conjugated to Dylight405 (1:100, Jackson ImmunoResearch) for CART. To reveal BrdU immunoreactivity, sections were treated with 2.4N concentrated HCl solution for 30 minutes at room temperature and then neutralized by 0.1M sodium tetraborate ($Na_2B_4O_7{\cdot}10H_2O$, two washes, 5 min each). The sections were then processed for BrdU immunohistochemistry with primary rat anti-BrdU (1:40, Abcam) antisera overnight, followed by donkey anti-rat Texas red (1:100, Jackson ImmunoResearch) antisera for 2 hours incubation. EdU immunohistochemistry was then carried out according to the manufacturer's instruction (Click-iT® EdU Alexa Fluor 488 imaging kit, Life Technologies).

Sections from the fourth series were processed for growth fraction analysis by Ki67 immunohistochemistry. Briefly, sections were subjected to antigen retrieval by incubation in 0.01 M citrate buffer, pH 6.0 at 95°C for 10 minutes followed by incubation overnight in

primary antisera against Ki67 (rabbit anti-Ki67, 1:200, Thermo Scientific), TH and Sox10 for E10.5–12.5 or PNMT for E13.5–16.5. The bound antisera were visualized after 2 hours incubation with secondary antisera: donkey anti-rabbit DyLight 594, donkey anti-chicken FITC and donkey anti-sheep Alexa Flour 647. The section were then washed and incubated with rabbit anti-CART antisera. Donkey anti-rabbit Biotin and streptavidin conjugated to Dylight405 were used to reveal CART immunofluorescence. Note that rabbit antisera were used together on the same sections for both Ki67 and CART. It was found that applying the Ki67 primary and secondary first, followed by washing and then the CART primary and secondary resulted in no significant crossing over of the secondary antisera. This could be confirmed because the different cellular localizations (nuclear vs. cytoplasmic) allowed us to discern whether secondary antisera were labelling only one or both rabbit primary antisera. To further confirm the growth fraction analysis, a separate set of sections was processed for identification of mitotic cells by phosphohistone-3 (PH3) immunohistochemistry. Sections from E12.5 embryos were incubated overnight in primary antisera against PH3 and TH followed by 2 hours incubation with secondary antisera, donkey anti-rabbit DyLight 594 and donkey anti-chicken FITC. The sections were then washed and incubated with rabbit anti-CART antisera as described above. Donkey anti-rabbit Biotin and streptavidin conjugated to Dylight405 were used to reveal CART immunofluorescence. All sections were imaged on a Zeiss Meta 510 scanning confocal microscope and processed by Zeiss Image Browser (v4.0.0241, Carl Zeiss Microimaging).

Data analysis

Single optical confocal images were taken from 3–4 embryos transversely sectioned through the upper abdominal region. The images were taken after optimizing microscope settings to have a minimum number of pixels saturated using the inbuilt histogram software. Images were analyzed by ImageJ (v1.48u, National Institutes of Health) software coupled with the cell counting and marking plug-in (v2010.12.07, Kurt De Vos, University of Sheffield). A circular or oval region of interest (mean area 5.75 μm^2) was selected in the perinuclear cytoplasm of each cell and the fluorescence intensity in the channels representing TH and CART immunoreactivity recorded. Subsequent analysis then compared the ratio between TH and CART intensity within each cell or the raw intensity of TH or CART fluorescence using Prism 6 statistical software (version 6.0f, GraphPad Software).

For cell cycle dynamic analysis, cells were counted manually for Ki67 (marker of cycling cells), BrdU and EdU. The growth fractions were calculated as the proportion of Ki67+ cells in the total number of each cell type present in the image. The S-phase length was calculated using the number of cells that were in S-phase at the end of the two hour period (BrdU +/EdU+, double positive plus EdU+ only) versus those that left S-phase (BrdU+ only) using the formula: *2h×[(BrdU+;EdU+ plus EdU+) over BrdU+]*. The instantaneous labelling index was the proportion of cells in S-phase at the time of first S-phase marker injection, which was calculated as the Y interception of two labelling indexes, obtained at 30 minutes after first injection (i.e. EdU+ only and BrdU+;EdU+) and at 2.5 hour after the first injection (i.e. BrdU+ only, EdU+ only and BrdU+;EdU+). The cell cycle length was then calculated as S-phase × (Growth fraction/Labelling index). Each parameter was calculated as a mean value with standard error of the mean from 3–5 embryos. Statistically analysis was performed with

Prism 6 software using one way ANOVA followed by Tukey's test. In all cases from E13.5–16.5, the suprarenal ganglion and the adrenal chromaffin cells were defined by their anatomical segregation. At E12.5, neuroblasts and chromaffin cells were differentiated based on CART and TH-immunohistochemistry (see Results for details).

3D reconstruction

The topographical distribution of SA cells was investigated in serial transverse 20μm cryostat sections through the trunk region of embryos at E12.5. Sections were incubated for 48 hours with primary antisera (chicken anti-TH, 1:100, Millipore). The bound antisera were visualized after 4 hours incubation with secondary antisera (donkey anti-chicken, FITC 1:100, Jackson ImmunoResearch) and the nuclei were stained with bisbenzimide. Z-stacks with 4 optical slices per images were acquired from serial sections on a Zeiss Meta 510 scanning confocal microscope. A total of 160 serial optical slices of 5 μm thickness were obtained and reconstructed in IMARIS v6 software (Bitplane v6) into an 842 × 842 × 800 μm^3 three-dimensional image with the anatomical structures outlined with reference to bisbenzimide staining on every 4th slice.

Results

Differential Expression of Phenotypic Markers

Transverse sections of the upper abdominal cavity from E10.5-E16.5 mouse embryos were examined. We first analyzed E10.5 and E11.5 mice for Sox10 immunoreactivity, which marks migrating NC cells, and for TH, a marker of sympathoadrenal (SA) progenitor cells. At E10.5, Sox10 positive (+) cells were present around the dorsal aorta, but no TH+ cells were observed. At E11.5, the first TH+ cells appeared amongst the Sox10+ cells close to the dorsal aorta. Cells expressing both Sox10 and TH were not observed at any age.

By E12.5, TH+ cells were common around the dorsal aorta (Fig. 1B). Three-dimensional reconstructions of the topographical distribution of TH+ cells in the vicinity of the dorsal aorta were performed (Fig. 1D–I) to determine if separate masses of neuronal and chromaffin cell precursors could be identified. The main mass of TH+ cells appeared in the midline, level with the rostral half of the developing kidneys. Paired paravertebral sympathetic chains were present dorsolateral to the aorta, with TH+ cells extending ventrally from the chains to expand into large bilateral masses of cells ventrolateral to the aorta, which were sometimes continuous ventral to the aorta. The most ventral TH+ cells were often associated with a single midline artery originating from the ventral surface of the aorta. We were unable to distinguish sympathetic neuroblasts and chromaffin cells on anatomical grounds at E12.5.

We examined the distribution of CART in the adrenal region of E11.5 - E16.5 mice. A few TH+ SA cells showed granular CART-immunoreactivity at E11.5 in the area around the aorta. All CART+ cells also exhibited TH immunostaining, identifying them as SA cells. At E12.5, CART-immunoreactivity was prominent in 38.4% of TH+ cells around the aorta (Fig. 2E–H). The overall intensity of CART immunoreactivity tended to be relatively higher at this age compared to E13.5 and later. By E13.5, when sympathetic ganglia primordia were

distinct from the adrenal anlagen (Fig. 2I–L), CART-immunoreactivity was present in 91.2% of sympathetic neuroblasts in the developing suprarenal prevertebral ganglia. Cells forming the adrenal medulla were largely devoid of CART immunostaining, although there were some TH+ cells expressing high levels of CART located around the interface between the suprarenal ganglion and the adrenal medulla. This is the location reported previously for extra-adrenal chromaffin cells of the Organ of Zuckerkandl (Schober et al., 2013). In mice, the organ of Zuckerkandl is largest at birth and then regresses, and it is thought to be part of the extra-adrenal chromaffin system that secretes catecholamines into the foetal circulation. Sympathetic neurons from E14.5-E16.5 mice were also CART+, with the levels of CART-immunoreactivity tending to be lower at older ages (Fig. 2M–X). The results suggest that, as early as E12.5, sympathetic neurons and adrenal chromaffin cells may be phenotypically distinguishable based on CART expression.

As previously reported (Schober et al., 2013), the TH+ cells located around the dorsal aorta exhibited a range of TH immunostaining intensities. In E12.5 mice, cells with low intensity of TH immunoreactivity ($TH+_{LO}$) tended to be found closer to the aorta, while those with high intensity ($TH+_{HI}$) were more commonly found further away, although there was considerable intermingling of $TH+_{LO}$ and $TH+_{HI}$ cells across their distribution (Fig. 2F). At E12.5, the intensity of CART immunostaining was also inversely correlated with the level of TH-immunostaining in that $TH+_{LO}$ cells often showed CART immunostaining, while CART immunoreactivity was rarely detectable in $TH+_{HI}$ cells (Fig. 2E–H). The CART+ cells found outside the suprarenal ganglion in the location of the Organ of Zuckerkandl were $TH+_{HI}$/CART+.

Relative fluorescence intensities for CART and TH immunostaining were quantified at E12.5 (n = 3 embryos, 184 cells), when prevertebral ganglia and adrenal medullae were not anatomically distinct. When raw fluorescence scores were considered for 184 TH-IR cells ventrolateral to the aorta at E12.5 across 3 embryos on a 0–255 scale (0 = no fluorescence, 255, = maximum fluorescence), the 92 cells with the highest CART fluorescence intensity had a mean TH fluorescence intensity of 87.1 ± 6.6 and the median value was 71.9. In contrast, the 92 cells with the lowest CART fluorescence intensity had a mean TH fluorescence intensity of 151.9 ± 7.4 and median value of 145.7.

At E13.5, when separate sympathetic ganglia and adrenal medulla anlagen could be discerned, $TH+_{LO}$ cells were predominantly in sympathetic ganglia and $TH-_{HI}$ cells in the adrenal medullae. As a consequence, there was an increased frequency of neuroblasts in the suprarenal ganglion that were $TH+_{LO}$/CART+, and chromaffin cells in the adrenal medulla that were $TH+_{HI}$/CART-. When the ratios of raw TH/CART fluorescence intensities were ranked for 150 chromaffin cells and 150 neurons from three E13.5 mice, the top 87 cells with the highest TH/CART staining ratio (HIghest TH/LOwest CART) were all chromaffin cells (Fig. 3). TH-IR cells in the developing adrenal medullae had a median TH intensity of 218.9 and a mean of 188.8 ± 5.7 while TH-IR cells in the suprarenal ganglion were 85.8 and 122.2 ± 7.4 respectively. The corresponding figures for CART immunofluorescence was median 10.7, mean 12.7 ± 1.0 (adrenal medullae) and median 37.0 and mean 49.3 ± 3.7 (suprarenal ganglia).

At E14.5, a handful of chromaffin cells in the adrenal medulla expressed the enzyme phenylethanolamine-N-methyl-transferase (PNMT+). PNMT methylates noradrenaline to form adrenaline and is therefore a marker of mature adrenergic chromaffin cells. By E16.5, adrenal medullary chromaffin cells were noticeably larger and more tightly packed together and 60% of all chromaffin cells were PNMT+.

Cell cycle dynamics

The proliferative behaviours of neuroblasts and chromaffin cells were examined using Ki67 immunohistochemistry to identify actively cycling cells and to calculate the growth fractions (the proportion of cycling cells). Sox10+ cells, the only NC cell type present at E10.5, were nearly all (88%) actively cycling (Fig. 4A). By E11.5, the majority (62%) of Sox10+ cells were still cycling (Fig. 4A), but very few (12%) of TH+ SA cells were in the cell cycle (Fig 4D). Thus, differentiation down the SA lineage is accompanied by cell cycle withdrawal, as it is in the mouse stellate ganglion (Gonsalvez et al., 2010). Cell cycle length calculated from the growth fraction and double-label S-phase labelling of Sox10+ cells was around 9.5 h at E10.5, and was significantly increased to nearly double by E12.5 (ANOVA, $F = 8.454$, $p = 0.0086$, Fig. 4B). S-phase length of Sox10+ cells was around 2.5 h at E10.5 and increased significantly to 6.8 h at E12.5 (ANOVA, $F = 6.347$, $p = 0.0191$, Fig. 4C). Sox10+ cells were not examined after E12.5 as they then likely to include glial/sustentacular cells as well as progenitors.

At E12.5, cell cycle parameters were analysed separately for CART+ (presumptive neuroblasts) and CART- cells (presumptive chromaffin cells). Many (70%) CART+ neuroblasts had re-entered the cell cycle at E12.5 (based on Ki67 immunoreactivity), but then steadily withdrew from the cell cycle over the succeeding days until only 24% of the cells were cycling on E16.5 (Fig. 4D). In contrast, only a small minority (19%) of CART- (chromaffin) cells were in the cell cycle at E12.5 and this proportion changed little over the succeeding days to 22% at E16.5 (Fig. 4D). The differences in proliferative behaviour of neuroblasts and chromaffin cells were further confirmed by PH3 immunoreactivity, which identifies proliferative cells at mitosis (M-phase). While 6% of CART+ cells (neuroblasts) at E12.5 were in M-phase only 0.4% of CART- (chromaffin) cells were in M phase. A third measure confirming the relative paucity of cycling cells among CART- (chromaffin) cells could be seen in an analysis of BrdU staining from the material used to calculate cell cycle length. Whereas 44% of CART+ cells (neuroblasts) were positive two hours after BrdU injection, indicating they were in S-phase and hence cycling, only 9% of CART- (chromaffin) cells were similarly labelled.

Neuroblast cell cycle length increased significantly by E16.5 to 27 h (ANOVA, $F = 6.821$, $p = 0.0021$, Fig. 4E), while that of PNMT- chromaffin cells did not change significantly over this time.

PNMT+ chromaffin cells, which first appear at E14.5, had a low growth fraction (19%, Fig. 4D) and, like PNMT- chromaffin cells, changed little over the next two days. Cell cycle and S-phase lengths were similar for both classes of chromaffin cells and did not change systematically over the period from E12.5-E16.5 (Fig. 4E–F).

Discussion

Many aspects of the development of SA lineages have been well studied, including their origin, migratory route and cell fates (Unsicker et al., 2013; Lumb and Schwarz, 2015). However, the mechanisms behind the segregation of SA cells into chromaffin and neural cell fates are still unknown. Unlike other sublineages of the trunk neural crest that have cell fates specified during early development (Krispin et al., 2010; Shtukmaster et al., 2013), chromaffin cells and sympathetic neurons appear to segregate only after reaching the ventrolateral aspects of the abdominal aorta (Krispin et al., 2010). We show here that chromaffin cells and sympathetic neurons differentially express CART on E13.5. CART is also differentially expressed among sympathoadrenal cells at E12.5, prior to the anatomical segregation of the cells, which may reflect the separation of the two lineages at this age.

Our data showing differences in proliferative behaviours between chromaffin cells and neuroblasts at E12.5 also support the idea that the two lineages could have diverged by E12.5. SA cells appear to temporarily exit the cell cycle upon differentiation into a TH-expressing cell, but only TH+/CART+ neuroblasts re-enter the cell cycle in significant numbers at E12.5. The phenotypic and proliferative differences between neuroblasts and chromaffin cells are summarized in Figure 5. Finally, both CART expression and proliferative behaviour also correlate inversely with the level of TH expression. Cells with high levels of TH expression generally lack CART expression and are often out of the cell cycle. Cells with these characteristics are usually chromaffin cells. In contrast, sympathetic neuroblasts tend to have low levels of TH expression and high levels of CART expression.

TH staining intensity and CART expression as early lineage markers

We have shown that CART expression and the level of TH immunostaining can be used to identify neuroblasts from adrenal chromaffin cells at E13.5 and, possibly, at E12.5. Our results therefore support previous studies, which suggested the divergence of the chromaffin cells and sympathetic neurons has already started at E12.5 (Stubbusch et al., 2013). Of note, CART appeared in some cells at E11.5, so the time of divergence could occur even earlier than E12.5 for some cells. Heterogeneity in the intensity of TH immunostaining of SA progenitor cells has been previously reported with chromaffin cells showing stronger TH staining than ganglion cells (Schober et al., 2013). Our quantitative data showing higher TH immunostaining in chromaffin cells compared to most ganglion cells confirm this earlier study.

The widespread expression of CART in embryonic sympathetic neuroblasts and absence from adrenal chromaffin cells is different from its distribution in adult rodents, suggesting that CART expression is transient in some cells types. In adult rats, CART is very rare in sympathetic postganglionic neurons but is present in many noradrenergic adrenal chromaffin cells (Dun et al., 2000; Gonsalvez et al., 2010). Thus, while CART is not a general marker for mature postnatal sympathetic neurons, it is present in nearly all embryonic sympathetic neurons and could be useful in distinguishing them from developing adrenal chromaffin cells. The role of CART during development has not yet been examined, but it should be noted that in the developing autonomic nervous system, CART has reported only in rapidly proliferating cells; ENS neurons (Heanue and Pachnis, 2006) and, in the current study, in

sympathetic neuroblasts, but not in chromaffin cells, which are largely out of the cell cycle. Otherwise, information about developmental roles for CART is sparse. One recent study demonstrated that exogenous CART peptide does not appear to participate in the neuronal differentiation of PC12 cells (Nagelova et al., 2014). CART is also widespread in the developing zebra fish brain (Mukherjee et al., 2012), but disappears at later ages.

CART expression and the levels of TH join NF-M and SCG10 (Ernsberger et al., 2005; Stubbusch et al., 2013) as markers that distinguish between sympathetic neurons and chromaffin cells as they differentiate. The ability to identify these two cell types soon after differentiation should facilitate analyses of the molecular machinery and signaling mechanisms underlying the divergence.

Proliferative behavior during SA lineages development

The separation of adrenal medullary chromaffin and sympathetic neuron lineages by E12.5 was confirmed by differences in proliferative behaviours between the two cell types. While we did not detect any striking differences in cell cycle or S-phase lengths between the two cell types, they do exhibit different growth fractions. Most of the NC progenitors (Sox10+ cells) around the abdominal dorsal aorta transiently exit the cell cycle at E11.5 coincident with the first expression of TH. Most TH+ ganglion cells subsequently re-enter the cell cycle at E12.5. This behaviour is similar to that reported for neuroblasts in the mouse stellate ganglion at E11.5 (Gonsalvez et al., 2013) but, in contrast to the present study, in the stellate virtually all neuroblasts exited the cell cycle, not just the majority as here. The stellate also differed in that cells co-expressing TH with Sox10 were present whereas none were found in the present study. The differences could be due to differences between developing paravertebral and prevertebral ganglia or may reflect a more compressed timeline for the development of the suprarenal ganglion, as the timing for SA progenitors lags approximately a day behind more caudal parts of the embryo. In contrast to TH+ neurons in suprarenal ganglia, very few TH+/CART- chromaffin cells re-enter the cell cycle at E12.5 or later stages.

The growth of the sympathetic ganglion must differ markedly from that of the adrenal medulla as a consequence of the differences in growth fraction of TH+ cells. The ganglion grows quickly, as most neuroblasts initially continue to divide after differentiating (Rothman et al., 1978; Rohrer and Thoenen, 1987) and then, from E12.5, neuroblasts progressively exit the cell again, this time permanently. By this mechanism, the ganglion achieves its maximum size quickly, during late embryonic ages. On the other hand, the relatively low numbers of chromaffin cells remaining in the cell cycle will result in only slow growth, although a small subset of chromaffin cells continue to divide postnatally (Tischler et al., 1989). A 5-fold increase in adrenal chromaffin cell number between E13.5 and P0 have been reported in mouse (Huber et al., 2002). With the growth fraction and cell cycle length data found in the present study, the number of chromaffin cells that would be generated at each 24 h period from E13.5 until P0 have been estimated, using the formula *initial number of non-cycling cell + (number of cycling cell* $\times 2^{(doubling\ times)}$) ie. $(1-GF)n_i + [(GF)n_i \times 2^{(24hr/CCL)}]$. Starting from 3,000 of cells at E13.5 (based on Huber et al., 2002) and consider the PNMT+ and PNMT- cells separately, a total of 13,318 cells would be produced by P0, a

4.44-fold increase. This is in good agreement with the 5-fold increase found by Huber et al. 2002. Sox10 cells in the medulla are also likely to contribute to the growth of the adrenal medulla (Santana et al., 2012). The progression of SA progenitors into the distinct lineages that differ with respect to expression of TH level, CART, PNMT and percentage of cells progressing through the cell cycle are detailed in Figure 5.

The sympathoadrenal progenitor

If the common SA progenitor is represented by the cells that start to express TH at E11.5, then a common SA progenitor may only exist for around 24 h, as separate sympathetic neuroblasts and adrenal chromaffin lineages are possibly already present by E12.5. Most SA progenitors are initially non-cycling cells. Shtukmaster et al. (2013) showed that, in chickens, one SA cell can give rise to both lineages. Assuming the same is true in mice, then SA progenitors must re-enter the cell cycle after E11.5 to give rise to cells of both types. Alternatively, the specification of each lineage could occur after NC cells leave the neural tube but before they give rise to SA progenitors, in which case an SA progenitor could give rise to just one of the lineages.

References

Anderson DJ. 1993 Cell fate determination in the peripheral nervous system: The sympathoadrenal progenitor. Journal of Neurobiology 24:185–198. [PubMed: 8445387]

Anderson DJ. 1993 Molecular control of cell fate in the neural crest: the sympathoadrenal lineage. Annu Rev Neurosci 16:129–158. [PubMed: 8460888]

Anderson DJ. 1997 Cellular and molecular biology of neural crest cell lineage determination. Trends Genet 13:276–280. [PubMed: 9242050]

Anderson DJ, Axel R. 1986 A bipotential neuroendocrine precursor whose choice of cell fate is determined by NGF and glucocorticoids. Cell 47:1079–1090. [PubMed: 2877748]

Bronner-Fraser M 1994 Neural crest cell formation and migration in the developing embryo. FASEB J 8:699–706. [PubMed: 8050668]

Callahan T, Young HM, Anderson RB, Enomoto H, Anderson CR. 2008 Development of satellite glia in mouse sympathetic ganglia: GDNF and GFR alpha 1 are not essential. Glia 56:1428–1437. [PubMed: 18551627]

Caviness VS Jr., Goto T, Tarui T, Takahashi T, Bhide PG, Nowakowski RS. 2003 Cell output, cell cycle duration and neuronal specification: a model of integrated mechanisms of the neocortical proliferative process. Cereb Cortex 13:592–598. [PubMed: 12764033]

Cheffer A, Tarnok A, Ulrich H. 2013 Cell cycle regulation during neurogenesis in the embryonic and adult brain. Stem Cell Rev 9:794–805.

Cheung M, Chaboissier MC, Mynett A, Hirst E, Schedl A, Briscoe J. 2005 The transcriptional control of trunk neural crest induction, survival, and delamination. Dev Cell 8:179–192. [PubMed: 15691760]

Cuchillo-Ibanez I, Michelena P, Albillos A, Garcia AG. 1999 A preferential pole for exocytosis in cultured chromaffin cells revealed by confocal microscopy. FEBS Lett 459:22–26. [PubMed: 10508910]

Dun NJ, Dun SL, Kwok EH, Yang J, Chang J. 2000 Cocaine- and amphetamine-regulated transcript-immunoreactivity in the rat sympatho-adrenal axis. Neurosci. Lett 283:97–100. [PubMed: 10739884]

Ernsberger U, Esposito L, Partimo S, Huber K, Franke A, Bixby JL, Kalcheim C, Unsicker K. 2005 Expression of neuronal markers suggests heterogeneity of chick sympathoadrenal cells prior to invasion of the adrenal anlagen. Cell Tissue Res 319:1–13. [PubMed: 15565470]

Francis NJ, Landis SC. 1999 Cellular and molecular determinants of sympathetic neuron development. Annu. Rev. Neurosci 22:541–566. [PubMed: 10202548]

Gabella G 2001 Autonomic nervous system. eLS.

Gonsalvez DG, Cane KN, Landman KA, Enemoto H, Young HM, Anderson CR. 2013 Proliferation and cell cycle dynamics in the developing stellate ganglion. J. Neurosci 33:5969–5979. [PubMed: 23554478]

Gonsalvez DG, Kerman IA, McAllen RM, Anderson CR. 2010 Chemical coding for cardiovascular sympathetic preganglionic neurons in rats. J Neurosci 30:11781–11791. [PubMed: 20810898]

Gonsalvez DG, Li-Yuen-Fong M, Cane KN, Stamp LA, Young HM, Anderson CR. 2014 Different neural crest populations exhibit diverse proliferative behaviors. Devel Neurobiol.

Heanue TA, Pachnis V. 2006 Expression profiling the developing mammalian enteric nervous system identifies marker and candidate Hirschsprung disease genes. Proceedings of the National Academy of Sciences of the United States of America 103:6919–6924. [PubMed: 16632597]

Huber K 2006 The sympathoadrenal cell lineage: specification, diversification, and new perspectives. Dev. Biol 298:335–343. [PubMed: 16928368]

Huber K, Combs S, Ernsberger U, Kalcheim C, Unsicker K. 2002 Generation of neuroendocrine chromaffin cells from sympathoadrenal progenitors: beyond the glucocorticoid hypothesis. Ann. N. Y. Acad. Sci 971:554–559. [PubMed: 12438182]

Huber K, Kalcheim C, Unsicker K. 2009 The development of the chromaffin cell lineage from the neural crest. Auton Neurosci 151:10–16. [PubMed: 19683477]

Huber K, Karch N, Ernsberger U, Goridis C, Unsicker K. 2005 The role of Phox2B in chromaffin cell development. Dev Biol 279:501–508. [PubMed: 15733675]

Kannan CR. 1986 Anatomy of the adrenal glands In: Essential Endocrinology: A Primer for Nonspecialists. Springer US p 233–234.

Krispin S, Nitzan E, Kalcheim C. 2010 The dorsal neural tube: a dynamic setting for cell fate decisions. Dev Neurobiol 70:796–812. [PubMed: 20683859]

Krispin S, Nitzan E, Kassem Y, Kalcheim C. 2010 Evidence for a dynamic spatiotemporal fate map and early fate restrictions of premigratory avian neural crest. Development 137:585–595. [PubMed: 20110324]

Landis SC, Patterson PH. 1981 Neural crest cell lineages. Trends in Neurosciences 4:172–175.

Langley K, Grant NJ. 1999 Molecular markers of sympathoadrenal cells. Cell Tissue Res. 298:185–206. [PubMed: 10550645]

Lumb R, Schwarz Q. 2015 Sympathoadrenal neural crest cells; The known, unknown and forgotten. Develop. Growth Differ

Morikawa Y, D'Autreaux F, Gershon MD, Cserjesi P. 2007 Hand2 determines the noradrenergic phenotype in the mouse sympathetic nervous system. Dev Biol 307:114–126. [PubMed: 17531968]

Mukherjee A, Subhedar NK, Ghose A. 2012 Ontogeny of the cocaine- and amphetamine-regulated transcript (CART) neuropeptide system in the brain of zebrafish, Danio rerio. J Comp Neurol 520:770–797. [PubMed: 22009187]

Nagelova V, Pirnik Z, Zelezna B, Maletinska L. 2014 CART (cocaine- and amphetamine-regulated transcript) peptide specific binding sites in PC12 cells have characteristics of CART peptide receptors. Brain Res 1547:16–24. [PubMed: 24378198]

Pattyn A, Morin X, Cremer H, Goridis C, Brunet JF. 1999 The homeobox gene Phox2b is essential for the development of autonomic neural crest derivatives. Nature 399:366–370. [PubMed: 10360575]

Reiprich S, Stolt CC, Schreiner S, Parlato R, Wegner M. 2008 SoxE proteins are differentially required in mouse adrenal gland development. Mol Biol Cell 19:1575–1586. [PubMed: 18272785]

Rohrer H 2011 Transcriptional control of differentiation and neurogenesis in autonomic ganglia. Eur J Neurosci 34:1563–1573. [PubMed: 22103414]

Rohrer H, Thoenen H. 1987 Relationship between differentiation and terminal mitosis: chick sensory and ciliary neurons differentiate after terminal mitosis of precursor cells, whereas sympathetic neurons continue to divide after differentiation. J. Neurosci 7:3739–3748. [PubMed: 3681410]

Rothman TP, Gershon MD, Holtzer H. 1978 The relationship of cell division to the acquisition of adrenergic characteristics by developing sympathetic ganglion cell precursors. Dev. Biol 65:322–341. [PubMed: 680364]

Saito D, Takase Y, Murai H, Takahashi Y. 2012 The dorsal aorta initiates a molecular cascade that instructs sympatho-adrenal specification. Science 336:1578–1581. [PubMed: 22723422]

Santana MM, Chung KF, Vukicevic V, Rosmaninho-Salgado J, Kanczkowski W, Cortez V, Hackmann K, Bastos CA, Mota A, Schrock E, Bornstein SR, Cavadas C, Ehrhart-Bornstein M. 2012 Isolation, Characterization, and Differentiation of Progenitor Cells from Human Adult Adrenal Medulla. Stem Cells Translational Medicine 1:783–791. [PubMed: 23197690]

Schober A, Krieglstein K, Unsicker K. 2000 Molecular cues for the development of adrenal chromaffin cells and their preganglionic innervation. European Journal of Clinical Investigation 30:87–90.

Schober A, Parlato R, Huber K, Kinscherf R, Hartleben B, Huber TB, Schutz G, Unsicker K. 2013 Cell loss and autophagy in the extra-adrenal chromaffin organ of Zuckerkandl are regulated by glucocorticoid signalling. J Neuroendocrinol 25:34–47. [PubMed: 23078542]

Shtukmaster S, Schier MC, Huber K, Krispin S, Kalcheim C, Unsicker K. 2013 Sympathetic neurons and chromaffin cells share a common progenitor in the neural crest in vivo. Neural Dev 8:12. [PubMed: 23777568]

Stanke M, Stubbusch J, Rohrer H. 2004 Interaction of Mash1 and Phox2b in sympathetic neuron development. Mol. Cell. Neurosci 25:374–382. [PubMed: 15033166]

Stubbusch J, Narasimhan P, Huber K, Unsicker K, Rohrer H, Ernsberger U. 2013 Synaptic protein and pan-neuronal gene expression and their regulation by Dicer-dependent mechanisms differ between neurons and neuroendocrine cells. Neural Development 8.

Tischler AS, Ruzicka LA, Donahue SR, DeLellis RA. 1989 Chromaffin cell proliferation in the adult rat adrenal medulla. Int J Dev Neurosci 7:439–448. [PubMed: 2816483]

Tsarovina K, Pattyn A, Stubbusch J, Muller F, Van Der Wees J, Schneider C, Brunet JF, Rohrer H. 2004 Essential role of Gata transcription factors in sympathetic neuron development. Development 131:4775–4786. [PubMed: 15329349]

Unsicker K, Huber K, Schober A, Kalcheim C. 2013 Resolved and open issues in chromaffin cell development. Mech Dev 130:324–329. [PubMed: 23220335]

Unsicker K, Huber K, Schütz G, Kalcheim C. 2005 The Chromaffin Cell and its Development In: Neurochem Res. Kluwer Academic Publishers-Plenum Publishers p 921–925.

Waring H 1936 Development of the adrenal gland of the mouse. Quarterly Journal of Microscopical Science 78:329–336.

Wildner H, Gierl MS, Strehle M, Pla P, Birchmeier C. 2008 Insm1 (IA-1) is a crucial component of the transcriptional network that controls differentiation of the sympatho-adrenal lineage. Development 135:473–481. [PubMed: 18094025]

Wurtman RJ, Axelrod J. 1966 Control of Enzymatic Synthesis of Adrenaline in the Adrenal Medulla by Adrenal Cortical Steroids. Journal of Biological Chemistry.

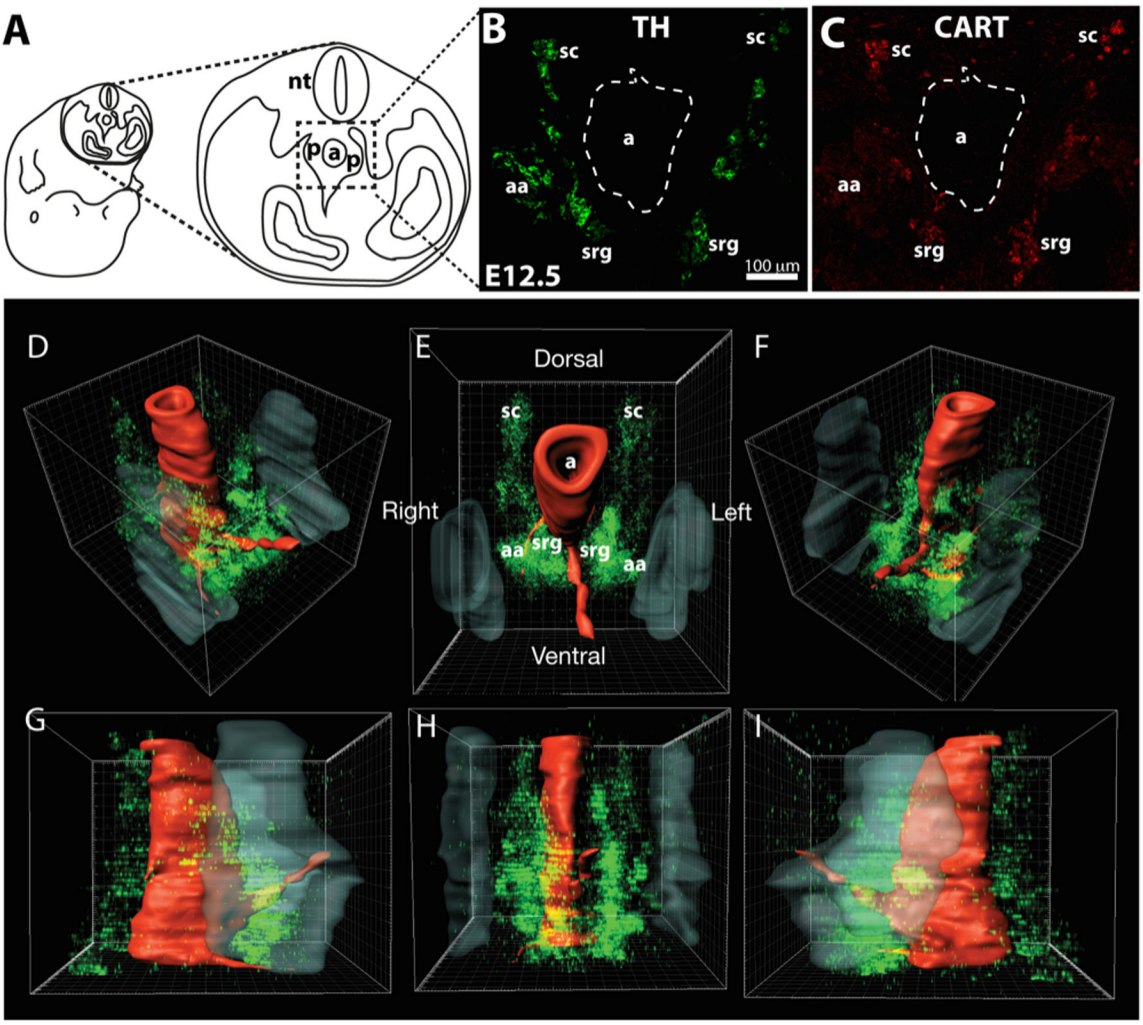

Figure 1.

Embryos were transversely sectioned through the upper abdominal cavity (A) and the region around the aorta (a), indicated by the dotted rectangle, imaged to include the sympathoadrenal primordia (p). B shows TH immunoreactivity in such a section at E12.5, while C shows CART immunoreactivity in the same section. Shown are the paravertebral sympathetic chain ganglia (sc), adrenal medullary anlagen (aa) and the prevertebral sympathetic suprarenal ganglia (srg). D-I shows a 3-dimensional reconstruction of the distribution of TH-immunoreactive sympathoadrenal cells (green) ventrolateral and ventral to the dorsal aorta in the sympathoadrenal primordial at E12.5. The dorsal aorta (red, a in E) and developing kidneys (grey) are outlined based on bisbenzimide staining. Views are right rostro-ventro-lateral (**D**), rostral (**E**), left rostro-ventro-lateral (**F**), right lateral (**G**), ventral (**H**) and left lateral (**I**). The paravertebral sympathetic chains (sc) are visible dorsal to the aorta as are the adrenal anlagen (aa) and suprarenal sympathetic ganglia (srg).

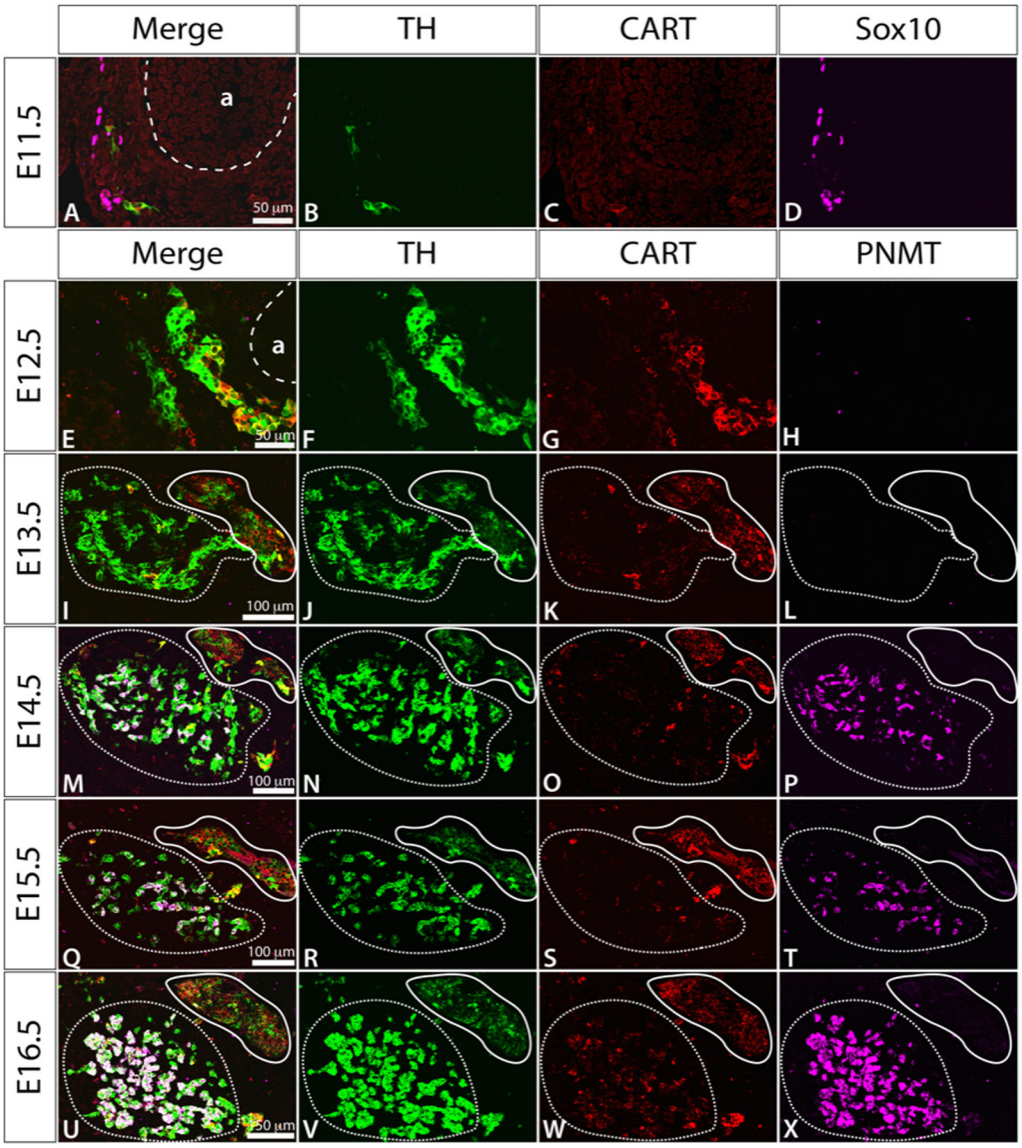

Figure 2.

Immunostaining of transverse sections through the adrenal region of mouse embryos at E11.5-E16.5, showing TH (green), CART (red) and Sox10 (magenta) at E11.5 and TH (green), CART (red) and PNMT (magenta) at E12.5-E16.5. In E13.5-E16.5, in prevertebral suprarenal ganglion is outlined in a solid line and the adrenal medulla in a dashed line. For orientation, each image represents a region equivalent to the lower left portion of figure 1C. “a” in A and E is the dorsal aorta.

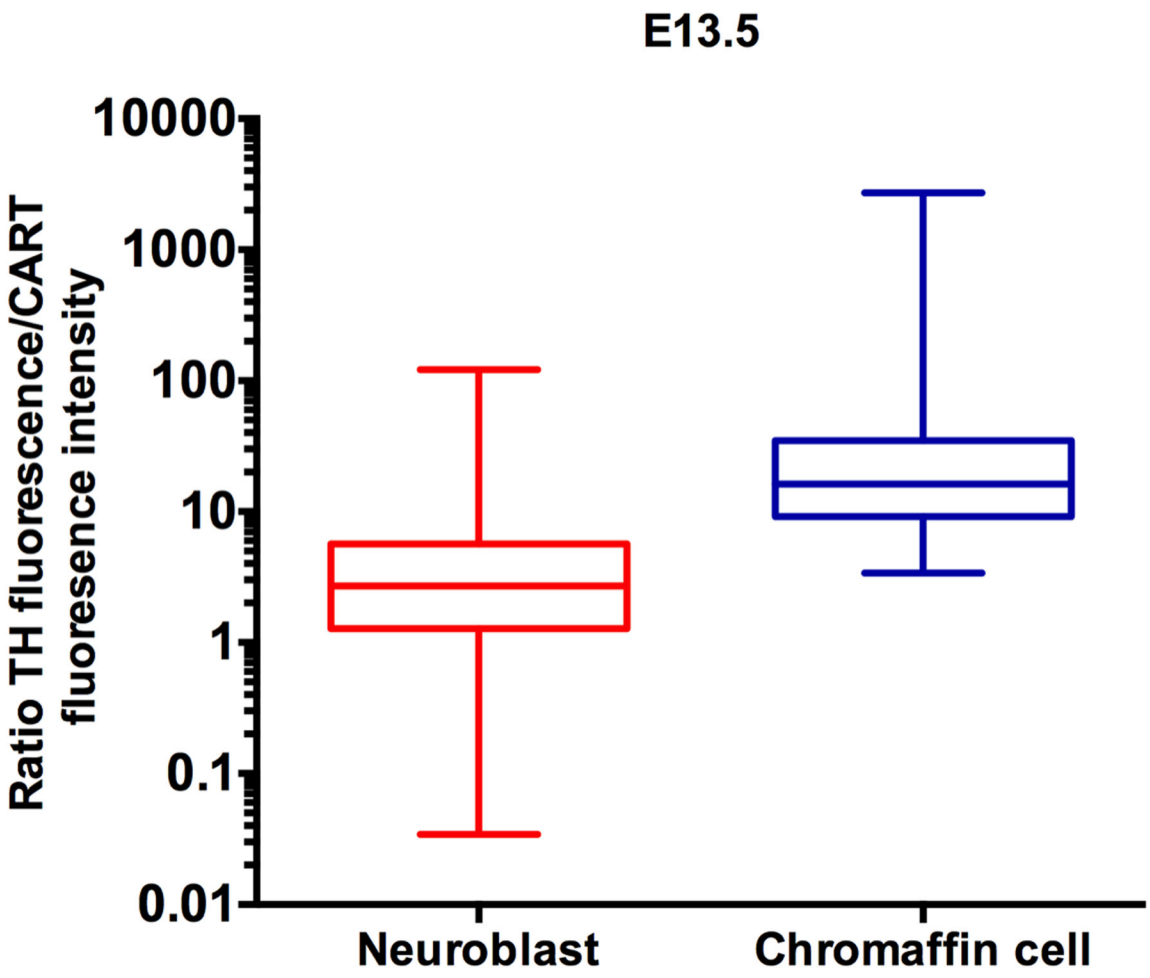

Figure 3.

Box and whiskers plot of ratio of TH-IR intensity over CART-IR intensity for neuroblasts and chromaffin precursor cells from a total of 3 mouse embryos at E13.5. Each plot shows the median value, the 25th and 75th percentile and the minimum and maximum values. Note the logarithmic Y-axis.

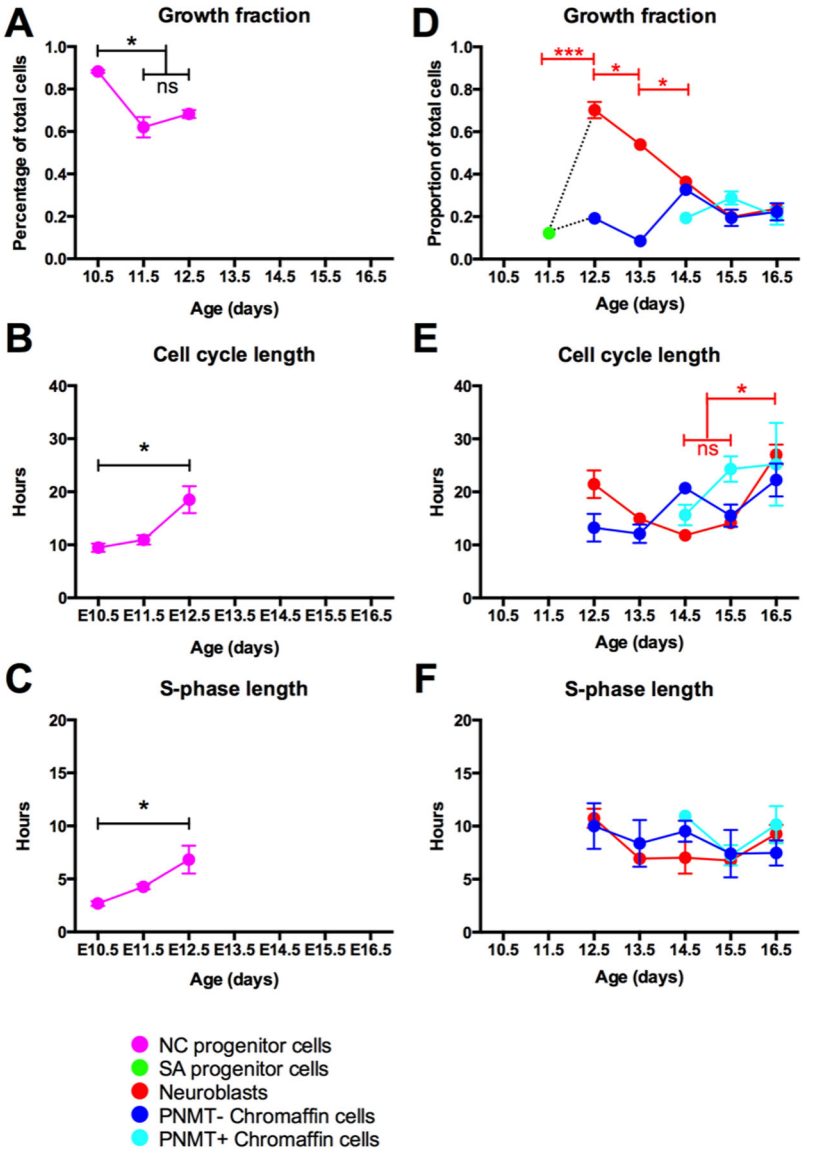

Figure 4.

Cell cycle parameters for developing mouse sympathetic ganglia and adrenal medulla from E10.5-E16.5. Plots record mean growth fractions (A and D), cell cycle lengths (B and E) and S-phase lengths (C and F) ± standard error of the mean. **A-C**, Data for Sox10+ neural crest progenitor cells from E10.5-E12.5. At E10.5, only Sox10 NCCs are present in the ganglion. At E11.5-E12.5, both Sox10+ NCCs are present with TH+ sympathoadrenal (SA) cells. Sox10+ cells are not shown after E12.5 as Sox10+ cells then include glial/sustentacular cells as well as NCCs. **D-F,** Data for SA cells, suprarenal ganglion (SRG) neuroblasts and chromaffin cells with (+) and without (−) PNMT from E11.5-E16.5. On E11.5, SA cells were identified by expression of TH; on E12.5 SRG neuroblasts were identified by expression of CART; on E13.5–16.5, SRG neuroblasts were identified by location in distinct SRG. Note the re-entry of cells into the cell cycle on E12.5 and the steady withdrawal thereafter. At E12.5, chromaffin cells were identified by presence of TH and absence of

CART-IR; at E13.5–16.5, chromaffin cells were present in a distinct adrenal medulla. In each graph, asterisks indicate pairs of means that were significantly different using one-way ANOVA followed by Tukey's test (*, $p < 0.05$; **, $p < 0.01$; ***, $p < 0.001$). NS, not significantly different. In D and E, only values for neuroblasts (red plot) were significantly different. Note that no CCL or S-phase length could be calculated for E11.5 SA cells as there were too few cells in the cell cycle.

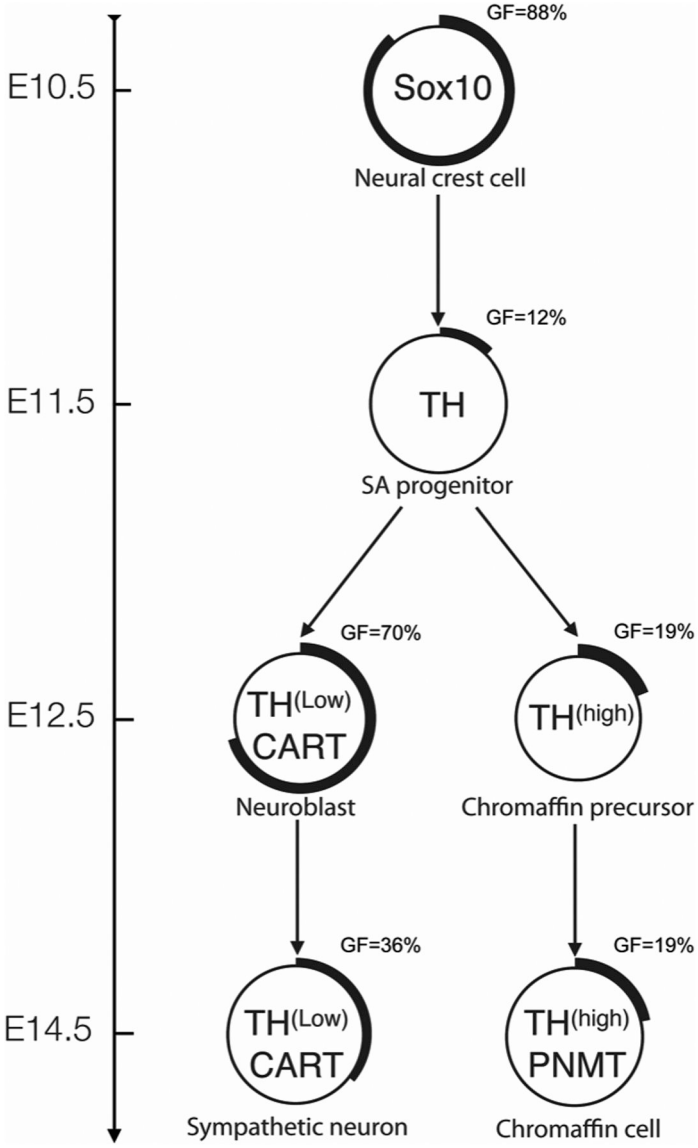

Figure 5.

Summary of phenotypic marker expression patterns and proliferation behavior during SA development. The neural crest-derived progenitor cells express Sox10 and are highly proliferative at E10.5. The percentage of cells in each population actively cycling is visually represented by the proportion of the outer ring that is thickened and also reported as growth fraction (GF) = x. At E10.5, in response to the BMPs released from the dorsal aorta, neural crest cells differentiate as bipotential SA progenitor cells, withdraw from the cell cycle and start expressing TH. On E12.5, two lineages have arisen; chromaffin cells can be distinguished from neuroblasts by a lack of CART expression, low intensity immunoreactivity for TH, and a low frequency of participation in the cell cycle. By E14.5, in the suprarenal ganglion primordia, neuroblasts are starting to withdraw from the cell cycle. In the adrenal medulla, significant numbers of TH^+ chromaffin cells start expressing PNMT while most cells remain out of the cell cycle.